



A novel method for combating dispersion induced power fading in dispersion compensating fiber

Lebedev, Alexander; Vegas Olmos, Juan José; Iglesias Olmedo, Miguel; Forchhammer, Søren; Tafur Monroy, Idelfonso

Published in:
Optics Express

Link to article, DOI:
[10.1364/OE.21.013617](https://doi.org/10.1364/OE.21.013617)

Publication date:
2013

Document Version
Publisher's PDF, also known as Version of record

[Link back to DTU Orbit](#)

Citation (APA):
Lebedev, A., Vegas Olmos, J. J., Iglesias Olmedo, M., Forchhammer, S., & Tafur Monroy, I. (2013). A novel method for combating dispersion induced power fading in dispersion compensating fiber. *Optics Express*, 21(11), 13617-13625. <https://doi.org/10.1364/OE.21.013617>

General rights

Copyright and moral rights for the publications made accessible in the public portal are retained by the authors and/or other copyright owners and it is a condition of accessing publications that users recognise and abide by the legal requirements associated with these rights.

- Users may download and print one copy of any publication from the public portal for the purpose of private study or research.
- You may not further distribute the material or use it for any profit-making activity or commercial gain
- You may freely distribute the URL identifying the publication in the public portal

If you believe that this document breaches copyright please contact us providing details, and we will remove access to the work immediately and investigate your claim.

A novel method for combating dispersion induced power fading in dispersion compensating fiber

Alexander Lebedev,* J. J. Vegas Olmos, Miguel Iglesias, Søren Forchhammer, and Idelfonso Tafur Monroy

DTU Fotonik, Dept. of Photonics Engineering, DTU, Technical University of Denmark, Kgs. Lyngby, Denmark
*alele@fotonik.dtu.dk

Abstract: We experimentally investigate the performance of 60 GHz double sideband (DSB) radio over fiber (RoF) links that employ dispersion compensating fiber (DCF). Error free transmission of 3 Gbps signals over 1 m of wireless distance is reported. In order to overcome experimentally observed chromatic dispersion (CD) induced power fading of radio frequency (RF) signal, we propose a method for improvement of RF carrier-to-noise (C/N) ratio through introduction of a degree of RF frequency tunability. Overall results improve important aspects of directly modulated RoF systems and demonstrate the feasibility of high carrier frequency and wide bandwidth RF signals delivery in RoF links including DCF fiber. Error free performance that we obtain for 3 Gbps amplitude shift-keying (ASK) signals enables uncompressed high-definition 1080p video delivery.

©2013 Optical Society of America

OCIS codes: (060.2330) Fiber optics communications; (060.5625) Radio frequency photonics.

References and links

1. Cisco white paper, "Cisco visual networking index: global mobile data traffic forecast update, 2012-2017," (Cisco, 2012).
http://www.cisco.com/en/US/solutions/collateral/ns341/ns525/ns537/ns705/ns827/white_paper_c11-520862.pdf.
2. Ericsson white paper, "Traffic and market data report," (Ericsson, 2011).
<http://hugin.info/1061/R/1561267/483187.pdf>.
3. Ericsson white paper, "Heterogeneous networks," (Ericsson, 2012).
<http://www.ericsson.com/res/docs/whitepapers/WP-Heterogeneous-Networks.pdf>.
4. M. C. Parker, S. D. Walker, R. Llorente, M. Morant, M. Beltrán, I. Möllers, D. Jäger, C. Vázquez, D. Montero, I. Librán, S. Mikroulis, S. Karabetos, and A. Bogris, "Radio-over-fibre technologies arising from the building the future optical network in Europe (BONE) project," *IET Optoelectron.* **4**(6), 247–259 (2010).
5. C. Lim, A. Nirmalathas, M. Bakaul, P. Gamage, L. Ka-Lun, Y. Yizhu, D. Novak, and R. Waterhouse, "Fiber-Wireless Networks and Subsystem Technologies," *J. Lightwave Technol.* **28**(4), 390–405 (2010).
6. A. M. Zin, M. S. Bongsu, S. M. Idrus, and N. Zulkifli, "An overview of radio-over-fiber network technology," in *Proceedings of IEEE International Conference on Photonics*, (Institute of Electrical and Electronics Engineers, San Francisco, 2010), paper ICP2010–85.
7. R. Herschel and C. G. Schaeffer, "Architectures for multiband multi gbps radio-over-fiber systems," in *Proceedings of 12th ITG Conference on Photonic Networks* (Institute of Electrical and Electronics Engineers, Leipzig, Germany, 2011), paper 24.
8. Vubiq specification datasheet, "60 GHz receiver waveguide module," (Vubiq, 2013).
<http://www.vubiq.com/pdf/Data%20Sheet%20V60RXWG2%20rev1.3.pdf>.
9. WirelessHD white paper, "WirelessHD Specification Version 1.1 Overview," (WirelessHD, 2010).
<http://www.wirelesshd.org/pdfs/WirelessHD-Specification-Overview-v1.1May2010.pdf>.
10. Siversima white paper, "MM-wave converter series for high capacity wireless transfer," (Siversima, 2010).
http://www.siversima.com/wp-content/uploads/2011/10/high-capacity-wireless-transfer_111010.pdf.
11. R. Hofstetter, H. Schmuck, and R. Heidemann, "Dispersion effects in optical millimeter-wave systems using self-heterodyne method for transport and generation," *IEEE Trans. Microw. Theory* **43**(9), 2263–2269 (1995).
12. K. Kitayama, "Ultimate performance of optical DSB signal-based millimeter-wave fiber-radio system: effect of laser phase noise," *J. Lightwave Technol.* **17**(10), 1774–1781 (1999).
13. A. Stohr, K. Kitayama, and T. Kuri, "Fiber-length extension in an optical 60-GHz transmission system using an EA-modulator with negative chirp," *IEEE Photon. Technol. Lett.* **11**(6), 739–741 (1999).

14. A. Ng'oma, Sh. Po-Tsung, J. George, F. Annunziata, M. Sauer, L. Chun-Ting, J. Wen Jr., Jyehong, and S. Chi, "21 Gbps OFDM wireless signal transmission at 60 GHz using a simple IMDD radio-over-fiber system," Conference on Optical Fiber Communication, collocated National Fiber Optic Engineers Conference (Optical Society of America, 2010), paper OTuF4.
15. M. Weiß, "60 GHz photonic millimeter-wave communication systems," PhD dissertation, University of Duisburg-Essen, 2010.
16. H. Sun, M. C. Cardakli, K.-M. Feng, J.-X. Cai, H. Long, M. I. Hayee, and A. E. Willner, "Tunable RF-powerfading compensation of multiple-channel double-sideband SCM transmission using a nonlinearly chirped FBG," *IEEE Photon. Technol. Lett.* **12**(5), 546–548 (2000).
17. B. Hraimel, Zh. Xiupu, M. Mohamed, and W. Ke, "Precompensated optical double-sideband subcarrier modulation immune to fiber chromatic-dispersion-induced radio frequency power fading," *J. Opt. Commun. Netw.* **1**(4), 331–342 (2009).
18. H. Sotobayashi and K. Kitayama, "Cancellation of the signal fading for 60 GHz subcarrier multiplexed optical DSB signal transmission in nondispersion shifted fiber using midway optical phase conjugation," *J. Lightwave Technol.* **17**(12), 2488–2497 (1999).
19. A. Lebedev, J. J. Vegas Olmos, X. Pang, S. Forchhammer, and I. Tafur Monroy, "Demonstration and comparison study for V- and W-band real-time high-definition video delivery in diverse fiber-wireless infrastructure," *Fiber Integrated Opt.* **32**(2), 93–104 (2013).
20. T. T. Pham, A. Lebedev, M. Beltrán, X. Yu, R. Llorente, and I. Tafur Monroy, "Combined singlemode/multimode fiber link supporting simplified in-building 60-GHz gigabit wireless access," *Opt. Fiber Technol.* **18**(4), 226–229 (2012).
21. J. Ma, J. Yu, C. Yu, X. Xin, J. Zeng, and L. Chen, "Fiber dispersion influence on transmission of the optical millimeter-waves generated using LN-MZM intensity modulation," *J. Lightwave Technol.* **25**(11), 3244–3256 (2007).
22. G. Hilt, "Optical transmission and upconversion of microwave signals in radio-over-fiber telecommunication Systems," PhD dissertation, L'institut National Polytechnique De Grenoble, (1999).
23. H. Schmuck, "Comparison of optical millimetre-wave system concepts with regard to chromatic Dispersion," *Electron. Lett.* **31**(21), 1848–1849 (1995).
24. U. Gliese, S. Norskov, and T. N. Nielsen, "Chromatic dispersion in fiber-optic microwave and millimeter wave links," *IEEE Trans. Microw. Theory* **44**(10), 1716–1724 (1996).

1. Introduction

The introduction of diverse bandwidth-demanding services requires an upgrade of current networks in order to provide higher bitrates for the end-user. Traffic generated by wireless/mobile services is predicted to grow at a fast pace with dominant applications such as data, file sharing, video, voice over internet protocol (VOIP) and gaming [1, 2]. Video traffic is predicted to increase at a highest annual growth rate compared to other services (taking up more than 70 percent of the overall traffic) [1].

In this work, we study the performance of heterogeneous links, which include fiber and wireless spans. In a recent report on heterogeneous networks [3], the use of distributed antenna systems (DAS) architecture is suggested in order to provide wired infrastructure for wireless traffic generated by the end-user, where antennas are located very densely with one antenna covering several rooms or even a single room. Among the physical layer fiber optic wired-wireless communication solutions for DAS network architecture, radio over fiber (RoF) stands out by addressing two important requirements: the need to simplify a remote antenna unit (RAU), potentially providing a solution only with passive components, and the need to centralize the signal processing at the common point for the optical and the electrical signal. An overview of RoF technology principles, advantages and recent advances can be found in [4–7].

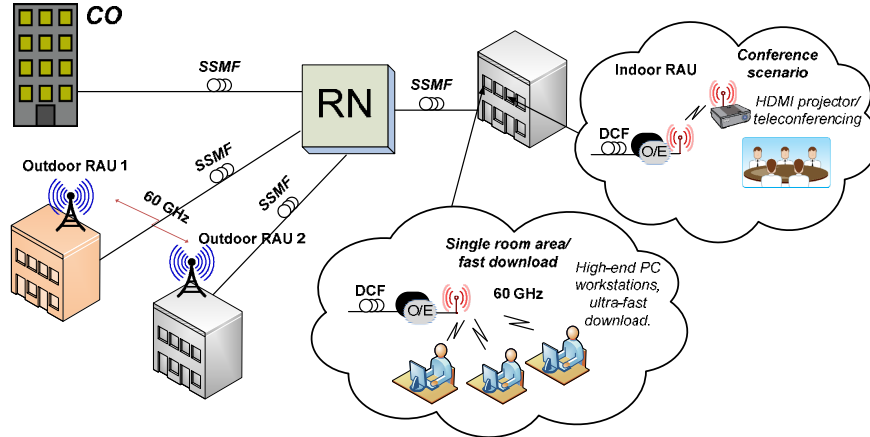


Fig. 1. Network scenario for 60 GHz RoF system. RAU: remote antenna unit, CO: central office, O/E: optical to electrical conversion, RN: remote node, DCF: dispersion compensating fiber, SSMF: standard single mode fiber.

Recent developments in component miniaturization have led to the appearance of commercially available solutions of 60 GHz up- and down-conversion integrated modules [8–10]. In order to provide seamless infrastructure for the electrical RF signal transfer between the central office (CO) and the RAU, we suggest that future fiber networks will need to transport the 60 GHz signals through the fiber span by means of direct intensity modulation of the lightwave that imposes double sideband (DSB) modulation on the carrier. Work on RoF DSB transmission has been widely reported, including methods to overcome the drawbacks of DSB modulation [11–13] and more recently reporting on ultra high bitrate wireless transmission (21 Gbps) through 500 meters of fiber [14]. Alternatives for DSB modulation, namely optical single sideband (OSSB) modulation and double sideband modulation with suppressed carrier (DSB-SC), have been studied and used extensively for RoF setups due to their increased tolerance against impairments. However, there are drawbacks for these approaches, such as a high optical power loss when we bias at the minimum point on a transfer characteristic of the Mach-Zehnder modulators (MZM), as in case of DSB-SC modulation, or high degree of complexity and accuracy in the optical filtering as in case of OSSB modulation. A thorough overview of photonic RF signal generation techniques can be found in [15].

In Fig. 1, we consider a network scenario for the 60 GHz fiber-wireless link that is capable of serving diverse applications. Our target application is real-time high definition (HD) uncompressed video transmission for business teleconferencing. Motivations for uncompressed video transmission include reduced latency and energy consumption. In this paper, we characterize the fiber-wireless system for a bitrate of 3 Gbps. The 3 Gbps bitrate would be sufficient to deliver 1080p uncompressed HD video. Systems of this bitrate that may also be alternatively used for ultra fast data download as indicated in the Fig. 1. Both of these applications may not be served by coaxial links combined with Wi-Fi if we consider the 3Gbps bitrate.

In the fiber architecture considered in this paper, photonic 60 GHz upconversion takes place at the remote node (RN). The metropolitan optical infrastructure is used to deliver the baseband signal from the CO to the RN. We consider that upconversion is made at the RN serving as an interface between metro and access parts of the network. In this scenario, a coil of dispersion compensating fiber (DCF) could be installed at the end-user site to compensate the effects of chromatic dispersion on a digitally modulated lightwave. The fiber-distributed 60 GHz wireless signals could subsequently serve in both indoor and outdoor wireless scenarios.

DCF is typically used for dispersion management in long reach optical fiber links. In this paper, we investigate the transmission of DSB modulated lightwave through DCF. Transmission of DSB signals in dispersive fiber media leads to appearance of phase change between the carrier and the sidebands that, after photomixing, results in RF carrier-to-noise (C/N) ratio degradation as a function of fiber distance and electrical oscillator frequency. A number of methods have been proposed for compensating RF C/N degradation that employ diverse fiber optics tools and electrical precompensation [13, 16–18]. In this paper, we show through experiment and simulation that the use of DCF for a lightwave modulated by an RF signal will be severely constrained by chromatic dispersion (CD) induced RF power fading. We then propose the algorithm to combat the RF power fading.

The novel contribution of this paper is twofold. First, this paper presents a 3 Gbps synchronous detection 60 GHz DSB RoF link operating below 10^{-9} BER level. The link's bitrate enables transmission of 1080p HD uncompressed video with an “off-the-shelf” hardware. Second, we study the transmission of DSB signals in DCF. Based on experimental results and modeling, we propose a method for improvement of the RF C/N ratio after the photomixing. Our proposed solution produces the reduction in CD induced degradation of RF C/N ratio and at the same time does not require a change in fiber infrastructure.

This paper is organized as follows: in Section 2 we present the laboratory setup and experimental performance assessment of the DSB 60 GHz DCF RoF link. In Section 3, we first present an analytical description for CD induced RF power fading in case of SMF and DCF based 60 GHz RoF links. Based on the observation of frequency-dependent behavior of CD induced RF C/N penalty for the DCF and SMF links, we propose a new algorithm for compensation of RF power fading. Finally, we provide a summary and conclusions in Section

2. Experimental setup for 60 GHz RoF employing DCF Fibers

The experimental setup of the 60 GHz DSB RoF system is presented in Fig. 2. A baseband data signal generated by a pulse pattern generator (PPG) producing a pseudorandom binary sequence (PRBS) with a word length of $2^{15}-1$ was mixed with a 58.24 GHz electrical signal from a factor-4 multiplied 14.56 GHz sinusoidal electrical signal. A lightwave carrier with a power of 6 dBm was generated by a laser diode (LD) of 1550 nm wavelength with less than 100 kHz line width. It was then modulated with the RF-upconverted signal through driving a Mach-Zehnder modulator (MZM) (35 GHz of -3 dB electrical bandwidth) biased at its quadrature point. An Erbium doped fiber amplifier (EDFA) was employed, followed by a 2 nm bandwidth optical bandpass filter (OBPF) to reject out-of-band amplified spontaneous emission (ASE) noise introduced by the EDFA. The fiber link was composed of either 50 or 100 meters of DCF. The dispersion parameter of the DCF fiber employed is -108 ps/(nm*km). After photodetection, we used a 16 dB gain 55-65 GHz bandwidth low noise amplifier (LNA) and a 28.7 dB gain 55-65 GHz bandwidth power amplifier (PA) to increase the signal power before radiation.

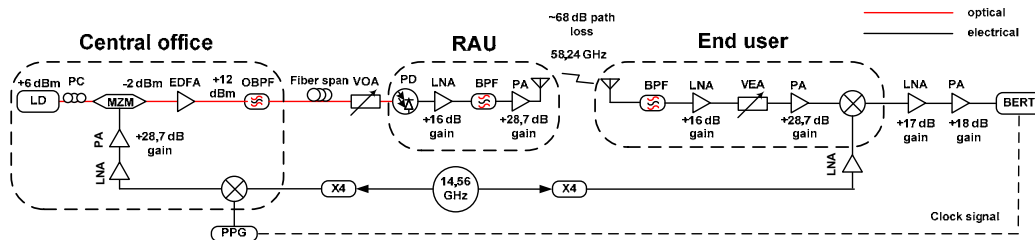


Fig. 2. Experimental setup of the 60 GHz DSB RoF system. LD: laser diode, PC: polarization controller, MZM: Mach-Zehnder modulator, EDFA: Erbium doped fiber amplifier, OBPF: optical bandpass filter, DCF: dispersion compensating fiber, VOA: variable optical attenuator, PD: photodiode, LNA: low noise amplifier, PA: power amplifier, BPF: bandpass filter, VEA: variable electrical attenuator, PPG: pulse pattern generator, BERT: bit error rate tester.

We employed commercially available high-directivity (25 dBi gain) horn antennas in order to improve the wireless link budget. 55-65 GHz bandpass filters (BPF) on the receiving and the transmitting side were used in order to reject out-of-band noise added by the photodiode (PD) and amplifiers. On the receiving side, we employed a variable electrical attenuator (VEA) to avoid the saturation of the amplifier. After reception of the signal, filtering and amplification, we downconverted the signal by means of mixing with the electrical oscillator synchronized in phase and frequency with the RF component of the detected signal. We employed a single electrical oscillator for the up- and down-conversion, however for a real-life implementation, when separate oscillators are implemented, phase locked loop (PLL) is required to be installed.

We employed a mixing technique to downconvert the data signal with the help of electrical oscillator in order to achieve 3 Gbps of bitrate for a wireless distance of 1 m. Alternative envelope detection techniques suffer from limitations on the bandwidth [19, 20]. We then used a baseband LNA (17 dB gain) and a PA (18 dB gain) to increase the peak-to-peak voltage level for the bit error rate tester (BERT) operation.

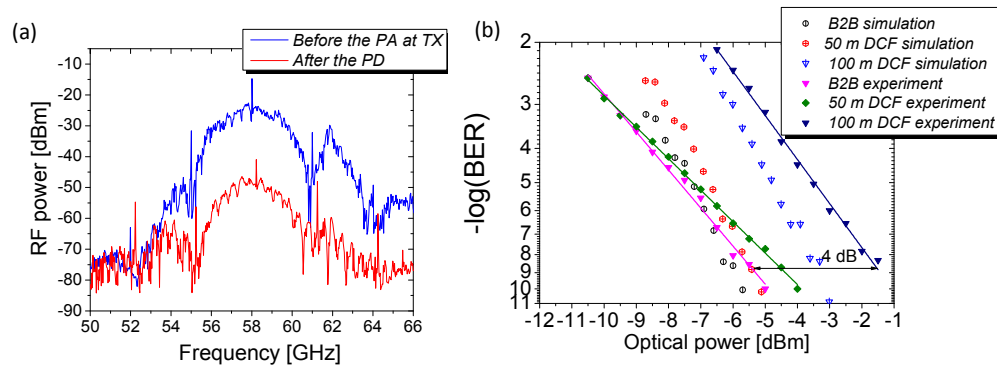


Fig. 3. (a) Experimentally measured electrical spectra of the signal before E/O and after O/E conversion, (b) BER curves as a function of the optical power.

Figure 3(a) shows the experimentally measured electrical spectrum of the signal before the PA at the CO side and after the PD at the optical receiver side. We observe a 30dB reduction of the signal power after transmission through the analog optical link; this reduction is overcome by using a cascade of the LNA and the PA before radiation.

The performance of the system in terms of BER is depicted in Fig. 3(b). We observe that the system performance is degraded significantly depending on the length of the fiber span; there is a 4 dB penalty between 50 m and 100 m spans. We attribute this effect to the distance-dependent CD induced RF C/N penalty. This severe penalty is caused due to the fact that we transmit through the fiber with high absolute value of the dispersion parameter. In Fig. 3(b), we present the results of both simulation and experiment of 60 GHz fiber-wireless system performance under a constraint of dispersion. Simulation was performed using the VPI software. The difference in the slope between the simulation and the experimental performance is attributed to the ambiguity in noise levels between the simulation and the laboratory setup. Simulation that we performed was focused on the estimate of CD induced RF C/N ratio degradation and certain aspects of the system performance have been simplified. The overall system noise sources include high frequency electrical amplifiers noise, shot noise of the PD, thermal noise, and ASE noise. Dispersion also contributes synchronization loss between sidebands and imposes deterioration on an eye-diagram as a function of fiber distance [21].

Analytical description of the CD induced RF C/N penalty and a novel algorithm to combat it are presented in the next section.

3. Method of improvement of RF C/N ratio through frequency tuning of the RF carrier

In this section, we propose an algorithm for compensation of RF power fading in DSB link based on observation of the increasing frequency periodicity of the RF carrier fading for increasing fiber link length. We present the improvement in C/N performance achievable with the software implementation of the frequency tuning algorithm.

Number of sophisticated solutions to combat the CD induced RF power fading have already been proposed and implemented in the field - such as employing transmitters with negative chirp [13], tunable compensation with Fiber Bragg Gratings (FBG) [16], through applying optimum electrical phase shift [17] and midway optical phase conjugation [18]. The novelty of our approach consists in the fact that we do not consider generation of a certain frequency, but we consider a transmission within a certain band for a given frequency shift of the local oscillator that is allowable, then we define the optimum frequency for transmission for a given fiber length and what effect it brings for the improvement of the impaired C/N ratio.

CD induced power fading effect is described analytically in references [22–24]; we only present the final formula as in [23]. Equation (1) reflects that C/N ratio of the RF signal recovered after the RoF link depends on dispersion parameter, fiber link length and frequency of the electrical oscillator.

$$P_{el}(t) \approx I_{PD}^2(t) \approx \cos^2[\varphi_d(\omega_m)] \approx \cos^2\left[\pi cDL(f_{RF}/f_c)^2\right] \quad (1)$$

where c is a light velocity, D is a dispersion parameter, in our calculations, we set it to 18 ps/(nm*km) for SSMF and -108 ps/(nm*km) for DCF, L is a fiber length, f_{RF} is a cyclic frequency of an electrical oscillator, which in our case is equal to 58.24 GHz, f_c is a frequency of a lightwave, we set it to 193.1 THz.

Equation (2) represents the value of RF C/N penalty in a logarithmic scale:

$$Penalty_{C/N} = 10 \log \left| \frac{X_{OUT}(f_c)_{fiber}}{X_{OUT}(f_c)_{nofiber}} \right| \quad (2)$$

$X_{OUT fiber}$ and $X_{OUT nofiber}$ is the signal power with and without fiber transmission.

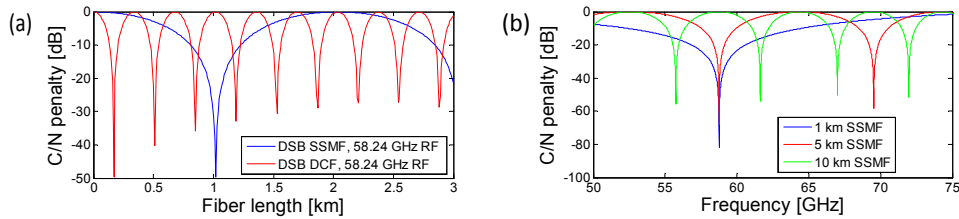


Fig. 4. Dispersion-induced power fading as a function of (a) fiber length for SSMF and DCF, (b) RF carrier frequency for SSMF.

In Fig. 4(a) we present the results of numerical calculation of CD induced RF power fading based on Eq. (1) and Eq. (2) for DCF and SSMF for a fixed frequency of the local oscillator. We see from Fig. 4(a) that the CD induced fading in case of DCF has higher periodicity along the fiber length. We chose the same RF carrier (58.24 GHz) for analytical estimation as was used throughout the experimental part of the work; it shows coherence with the experimental data where more severe constant power fading was observed in case of DCF. The first dip in C/N ratio for DCF occurs at 170 m length compared to 1020 meters for the first dip length for SSMF. The first -3 dB penalty occurs at 510 m and 85 m for SSMF and DCF respectively.

The Fig. 4(b) reflects the fact that there is a set of frequencies for a given fiber length that produces minimum CD induced RF C/N degradation. For example, as depicted in Fig. 4(b) 10 km SSMF span has 5 optimal frequencies in V-band range.

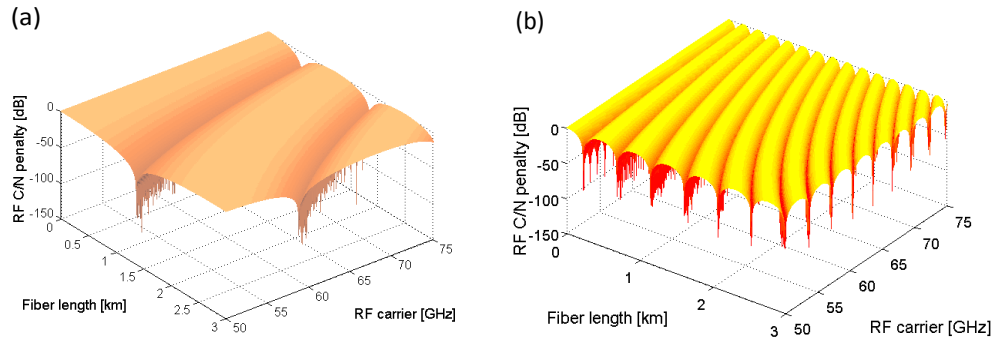


Fig. 5. Dispersion induced power fading as a function of frequency and fiber length for SSMF (a) and DCF (b).

In Fig. 5, we depict the surface plots for the combined effects of distance-dependent and frequency-dependent RF power fading in case of SSMF and DCF. It is visible that periodicity of fading for DCF is higher in both frequency domain and along the fiber length. We then present the algorithm to overcome CD induced RF power fading for a given bandwidth of local oscillator tuning.

Tunability in frequency domain is important notion to consider given that RF oscillators that are produced currently by the industry are frequency tunable, and thus the frequency of an oscillator can be adjusted in order to improve RF C/N ratio for a given length of deployed fiber. It is also important to note that the periodicity of the fading is increasing with the increase in fiber length, thus, for longer distances of fiber, we need less tuning bandwidth to obtain the same improvement in C/N ratio. At the same time, we also need to note from Fig. 4 and Fig. 5 that, with increase in the fiber length, the -3 dB bandwidth of minimum fading values for the signal decreases. Our numerical simulations indicate that a -3 dB bandwidth of 6 GHz occurs for V-band signals with this type of DCF in distances above 800m.

We make the following assumptions for the model: we do not have the prior knowledge of the fiber distance for the deployed link, and we have a low data rate link to transmit the control signals from the optical receiver to the optical transmitter. Low data rate link may be a part of a larger packet-based network, where the 60 GHz fiber-wireless connection serves as a backbone.

It is important that we have sufficient amount of bandwidth in the wireless part of the link to allow the frequency tunability without breaking the unlicensed frequency allocation borders. The range of frequencies allocated for unlicensed use around 60 GHz varies from country to country, for instance, in Europe the frequency is allocated within 57-66 GHz bandwidth [9]. According to [9], a channel bandwidth can occupy up to 2160 MHz. The bandwidth of a main lobe of our signal is approximately 6 GHz. However, the proposed algorithm will work also with lower bandwidth signals. In order to enable 3 Gbps error free transmission in 2160 MHz band defined by [9], QAM-16 modulation is necessary for a single carrier transmission.

The concept of the algorithm is as follows:

- 1) At the CO (or the RN depending on the scenario,) electrical oscillator frequency is set in a 60 GHz unlicensed band (our choice-58.24 GHz).

- 2) The RF is swept with an arbitrary step (we chose 0.01 GHz) at the transmitter and values of RF power after the photodiode are stored.
- 3) RF power values are sent to the transmitter through the low data rate channel, where the frequency that resulted in maximum RF power at the output of the photodiode is selected.

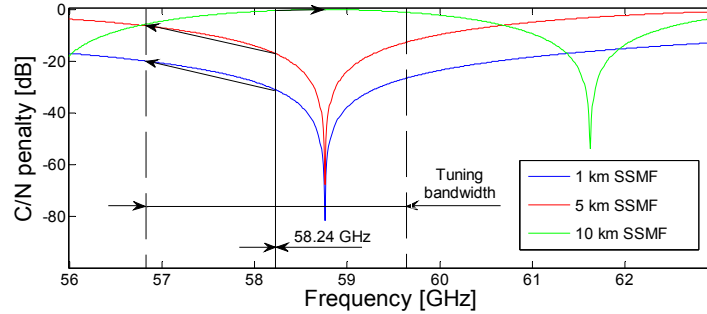


Fig. 6. An example of the algorithm performance for 1, 5 and 10 km of SSMF transmission.

Figure 6 is a close-up of a Fig. 4(b) where tuning is depicted for SSMF. Originally, frequency is set to 58.24 GHz. For 1 km and 5 km of fiber distance, the necessary frequency shift to improve the C/N ratio is the largest possible tuning shift (-1.4 GHz), however, for 10 km distance, the necessary shift is 0.52 GHz. The algorithm for DCF has the same principle of operation as depicted in Fig. 6.

Figure 7 and Fig. 8 depict the results of frequency-tuning based optimization under the constraints of tuning bandwidth (2.8 GHz as in commercially available module that was used for the experiment) and RF-spectrum allocation.

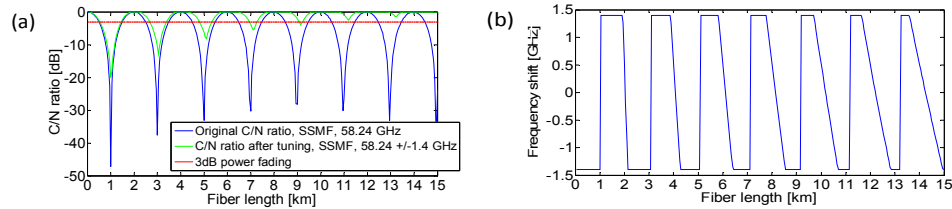


Fig. 7. (a) Improvement of C/N ratio with a frequency tuning method for SSMF, (b) the required frequency shift to produce the improvement of the C/N ratio for SSMF case.

It's important to note that the frequency tuning algorithm produces superior performance at longer lengths of fiber since as we may see from the Fig. 4(b) the frequency-dependent fading dips occur more often at longer spans of fiber. Our proposed method for CD induced RF power fading compensation brings performance at no more than 3 dB RF power penalty at the distance of around 11 km for SSMF and at the distance of 1.8 km for DCF fiber. We also see that, at lower fiber distances, maximum absolute carrier frequency shift is the preferred choice, but, as the distance increases, the algorithm selects the lower frequency shifts more often. It is due to the fact that the frequency periodicity of fading is increasing with distance that there is a smaller frequency shift required that can lead to a maximum possible improvement of RF C/N ratio inside of the tuning bandwidth.

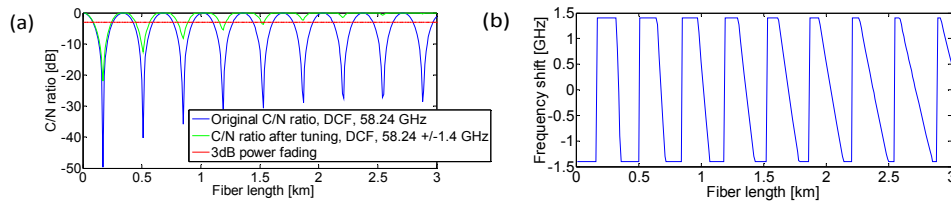


Fig. 8. (a) Improvement of C/N ratio with a frequency tuning method for DCF, (b) the required frequency shift to produce the improvement of the C/N ratio for DCF.

We show that although DCF fiber has more frequent occurrence of CD induced RF power fading, when we employ the algorithm for frequency tuning, we may achieve better performance for DCF fiber compared to the case of SSMF.

Future work includes a laboratory implementation that requires installation of automatically controlled V-band power meter storing the power values. Once the frequency is swept at the transmitter, the RF power values are stored at a power meter on the receiving side, they can then be communicated to the transmitter using an available uplink channel where the decision on appropriate frequency shift is made and a new frequency is set through the automatic control of the RF-generating board.

4. Conclusions

We experimentally demonstrated a 60 GHz DSB RoF synchronous detection link capable of transmitting 1080p uncompressed video. We studied CD induced RF degradation for DCF through experiment, simulation and analytical assessment. The experimental results have indicated severe degradation of RF carrier after photomixing in case of DCF deployment, which agrees well with simulation and analytical solution. Analytical results presented in this paper indicate that increase in absolute value of dispersion parameter, e.g. when we employ DCF, increases the periodicity of CD induced RF degradation. Based on experimental results and modeling, we then proposed an algorithm for frequency tuning of the electrical oscillator that uses an advantage of the wide 60 GHz bandwidth.

Acknowledgment

J. J. Vegas Olmos acknowledges the Marie Curie program for partly funding this research through the WISCON project.